engineering proceedings

MDPI

Proceeding Paper

Investigating the Terrain Complexity from ATL06 ICESat-2 Data for Terrain Elevation and Its Use for Assessment of Openly Accessible InSAR Based DEMs in Parts of Himalaya's †

Ashutosh Bhardwaj

Photogrammetry and Remote Sensing Department, Indian Institute of Remote Sensing, Dehradun 248001, India; ashutosh@iirs.gov.in; Tel.: +91-135-2524117

† Presented at the 8th International Electronic Conference on Sensors and Applications, 1–15 November 2021; Available online: https://ecsa-8.sciforum.net.

Abstract: Spaceborne sensors are now providing invaluable datasets for the Earth's surface studies. The Ice, Cloud, and land Elevation Satellite-2 (ICESat-2) with the Advanced Topographic Laser Altimeter System (ATLAS) was launched by NASA on 15 September 2018, to measure the elevation of the Earth's surface using a laser wavelength of 532 nm and pulse repetition frequency of 10 kHz giving a footprint of approximately 70 cm on the ground. The ICESat-2 datasets are used in this study for the visualization and investigation of the complex Himalayan terrain in the parts of the Kinnaur district and surroundings, which are prone to frequent landslides due to the geology of the region as observed during the recent landslide events. The ICESat-2 elevation datasets were compared with the openly accessible DEM datasets namely, ALOS PALSAR RTC HR (12.5 m) and TanDEM-X (90 m) at ICESat-2 footprint locations. The preprocessing of datasets was completed for selecting ICESat-2 footprints (Track ID: 325, 1270, 828, 386) at locations of high-quality datasets for analysis. The analysis of pre-processed 19,755 ICESat-2 footprints (out of 20,948 footprints) was performed with ALOS PALSAR RTC HR (12.5 m) and TanDEM-X (90 m) datasets. The visualization of the region in the Google earth and OpenAltimetry 3D viewer depicts that the mountain slopes are very steep indicating rugged terrain difficult to access and challenging for construction of transport facilities. The results of Track ID: 325, show that the range of elevations in ICESat-2 elevation values in the study area is from 3409.75 m to 5976.31 m. The standard deviation representing terrain ruggedness using ICESat-2 elevation values is found as 432.06 m. Considering higher accuracy ICESat-2 values for the difficult terrain as a reference, the mean error (ME), mean absolute error (MAE), and RMSE for TanDEM-X were found as 0.26 m, 12.92 m, and 17.4 m, respectively. Whereas the ME, MAE, and RMSE for ALOS PALSAR RTC HR DEM were found as 0.20 m, 9.50 m, and 13.88 m, respectively. Thus, for the study site, using ICESat-2 ATL06 products, ALOS PALSAR RTC HR DEM is found more suitable than TanDEM-X 90 m openly accessible datasets for any kind of application in such a terrain.

Keywords: LiDAR; ATLAS; DEM; ALOS PALSAR RTC HR; TanDEM-X; terrain ruggedness

check for updates

Citation: Bhardwaj, A. Investigating the Terrain Complexity from ATL06 ICESat-2 Data for Terrain Elevation and Its Use for Assessment of Openly Accessible InSAR Based DEMs in Parts of Himalaya's. *Eng. Proc.* **2021**, *10*, 65. https://doi.org/10.3390/ecsa-8-11327

Academic Editor: Stefano Mariani

Published: 1 November 2021

Publisher's Note: MDPI stays neutral with regard to jurisdictional claims in published maps and institutional affiliations.

Copyright: © 2021 by the author. Licensee MDPI, Basel, Switzerland. This article is an open access article distributed under the terms and conditions of the Creative Commons Attribution (CC BY) license (https://creativecommons.org/licenses/by/4.0/).

1. Introduction

Every topographic region has its advantages and disadvantages affecting socioeconomic wellbeing in the region. Some regions are prone to floods, forest fires, earthquakes, tsunami, landslides, and so on. The mountainous regions have always been a challenge for the dwellers due to the availability of resources and infrastructure. Different mountainous regions of the world face different challenges, such as snow avalanches, rockslides, shortage of oxygen in higher reaches, health facilities, etc. The higher reaches of Himalayas also have similar challenges due to their ruggedness making the terrain less convenient for dwellers. However, at the same time, it has pleasant weather and a scenic atmosphere around, making many locations a choice for tourists.

The major mountain ranges of the world include the Andes, the Rockies, the Great Dividing Range, the Transantarctic Mountains, the Ural Mountains, the Atlas Mountains, the Appalachian Mountains, the Himalayas, the Altai Mountains, the Western Ghats, the Alps, the Drakensberg, and the Aravalli Range, among others. Performing traditional surveys in these regions will be time-consuming and costly. ICESat-2 provides a good opportunity to study these mountains through its ATLAS instrument in addition to other remote sensing technologies. Landslides are common in the Alps [1,2], Himalayas [3,4], eastern Patagonian Andes [5], and other mountains of the world depending on the geology and weather conditions primarily while making the habitat more vulnerable in terms of both the dwellers, as well as the structures. The State of Conservation Index (SCIx), which serves as an input in a Spatial Multicriteria Evaluation (SMCE), was used to study the vulnerability of 60 cultural heritage objects in Georgia from landslides and avalanches [6].

Chen et al. (2020) have evaluated the accuracy of SRTM3 DEM using ICESat/GLAS data over Jiangxi province, China [7,8]. Zhang et al. (2021) analyzed 208 footprints of ICESat-2 ATL06 data and found that they have very high vertical and horizontal positioning accuracies. The average RMSE calculated for continuously operating reference stations (CORS) is 0.0846 m, and the corresponding RMSE for unmanned aerial vehicle (UAV) data is 0.1517 m [9]. Liu et al. (2020) found, in a study over steep terrain of the south-central Chinese province of Hunan, that the DEMs (SRTM-1 DEM, SRTM-3 DEM, ASTER GDEM2, AW3D30 DEM, and TanDEM-X 90-m DEM) provide the elevations higher than those of reference points [10]. A regional landslide inventory prepared with a focus on the Swiss and French Alps shows that the post-1970 portion of the database is more reliable, highlighted through an improved power–law relationship [11]. The week areas having fractured materials resting on steep slopes falls during landslides in the parts of the Appalachian Mountains, the Rocky Mountains, the Pacific Coastal Ranges, and some parts of Alaska and Hawaii [12]. Gracheva et al. (2009) studied the effects of landslides on archeological site Gruzinka (North Caucasus, Russia), including soil and minerals [13]. Wang et al. (2019) studied algorithms which included the influencing factors, namely, the signal-to-noise ratio (SNR), slope, vegetation height, and vegetation cover on the accuracy of ground elevation over the forest, tundra, and bare land areas in interior Alaska using airborne LiDAR data. The overall mean difference and RMSE values between the ground elevations are −0.61 m and 1.96 m, respectively. Whereas in the forest, tundra, and bare land scenarios, the mean differences are −0.64 m, −0.61 m, and −0.59 m, with RMSE values of 1.89 m, 2.05 m, and 1.76 m, respectively, which are quite acceptable for difficult terrains having a large influence of slope [7]. A recent event of a rockslide in Chamoli, Uttarakhand has also been studied by researchers extensively, such as Ronti site, Uttarakhand [14–16]. The Copernicus DEM is found better than other openly accessible DEMs (ALOS, ASTER, NASA, and SRTM) in all eight test areas, when tested against both LiDAR and ICESat-2 data [17]. Openly accessible DEMs (TanDEM-X, SRTM, ASTER, ALOS PALSAR, CartoDEM) and Radargrammetric DEM generated using RISAT-1 (C-band) SAR stereo pair were evaluated with ICESat-2 footprints for the highly vegetated Himalayan mountainous terrain of Dehradun and surroundings in Uttrakhand state, India [18]. The presented study focuses on the evaluation of two recent high-quality InSAR-based DEMs using spaceborne LiDAR data from the ICESat-2 mission. The study on the quality of DEMs is essential as DEMs play an important role in generating correct results from geographic information system (GIS) based modeling from inputs for any phenomenon using remote sensing techniques.

2. Study Area

The study area is part of Himachal Pradesh in India, which shares its borders with the union territories of Jammu and Kashmir and Ladakh towards its north, and with the states of Haryana towards the southwest, Uttarakhand to the southeast, Uttar Pradesh to the South, and with Punjab to the west (Figure 1). The study area includes parts of the Kinnaur district and its surroundings, where some of the heavy landslides have been reported recently in the mid of the year 2021 during monsoon season. The state of Himachal

Pradesh, including the study area, is characterized by an extremely undulating landscape, having several peaks and regions with extensive drainage networks consisting of various river systems.

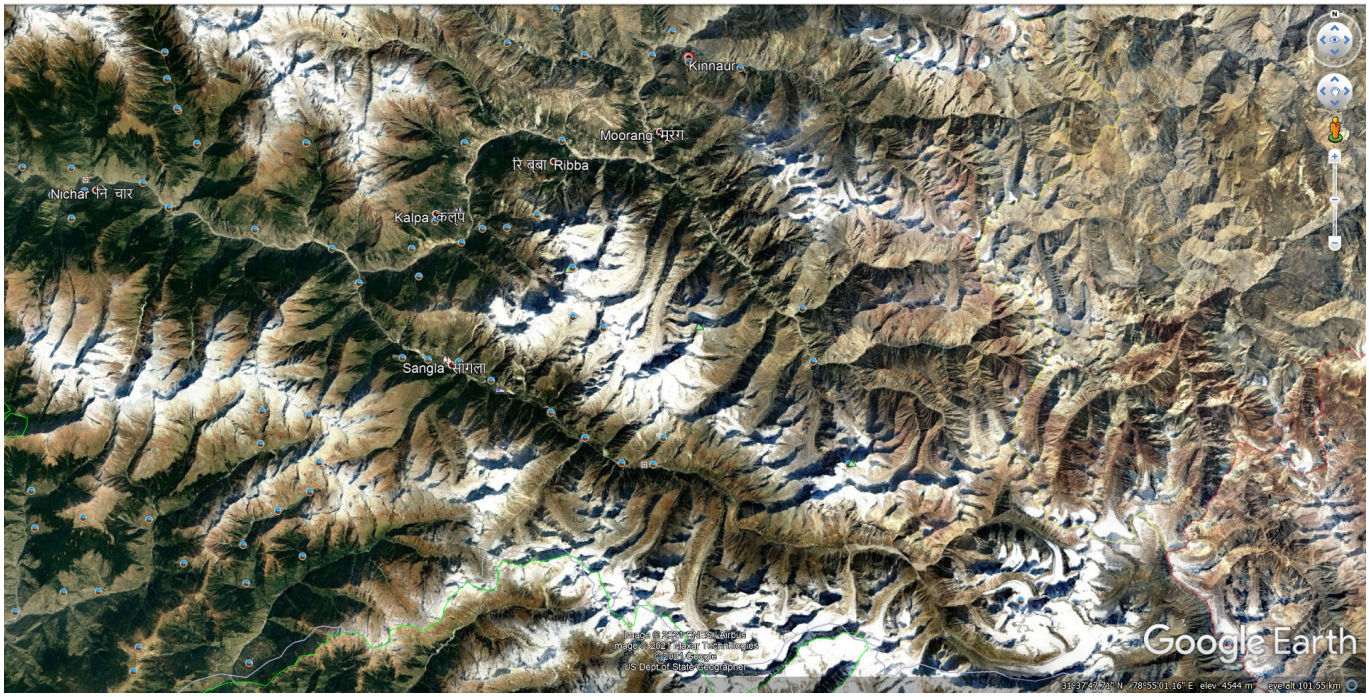

Figure 1. Study area.

3. Material

3.1. Openly Accessible DEMs

3.1.1. TanDEM-X 90

The TanDEM-X (90 m) DEM dataset was downloaded from the website platform provided by DLR (https://tandemx-90m.dlr.de (accessed on 4 August 2021)). The detailed specifications of TanDEM-X DEM products can be seen in the data guide provided by DLR (https://geoservice.dlr.de/web/dataguide/tdm90/#introduction (accessed on 4 August 2021)).

3.1.2. ALOS PALSAR RTC HR DEM

The radiometrically terrain corrected (RTC) products is a project of the Alaska Satellite Facility (ASF) that makes SAR data accessible to the user community at a high resolution (HR) of 12.5 m and a resolution of 30 m. The ALOS PALSAR RTC HR product (12.5 m) was used for the experiment (https://asf.alaska.edu/data-sets/sar-data-sets/alos-palsar/ (accessed on 4 August 2021)).

3.2. Spaceborne LiDAR Data (ICESat-2)

Ice, Cloud, and land Elevation Satellite-2 (ICESat-2) with ATLAS instrument was launched by NASA and measures the elevation of Earth's surface using laser wavelength of 532 nm and PRF of 10 kHz producing ~70 cm footprint on the ground. This dataset (ATL06) provides geolocated land-ice surface heights (above the WGS 84 ellipsoid, ITRF2014 reference frame), plus ancillary parameters that can be used to interpret and assess the quality of the height estimates.

4. Method

The ICESat-2 shapefiles were generated using the ICESat-2 (ATL06) Excel datasheets in ArcGIS software after preprocessing of ICESat-2 data for removal of outlier values resulting in 19,755 footprints (out of 20,948 footprints). The shapefile was used further to extract the elevation values from TanDEM-X and ALOS PALSAR RTC HR DEMs. Further, the extracted values from DEMs were tested against ICESat-2 elevation datasets in the WGS84 datum. Considering the data characteristics of openly accessible DEMs used in this study and the ICESat-2 data, the ICESat-2 elevation values after pre-processing are used as reference elevation for the computation of statistical measures. The preprocessing mainly includes the removal of outlier values from the datasets considering the terrain ruggedness and land use and cover (LULC). Statistics comprising of the mean error (ME), mean absolute error (MAE), and RMSE were computed for both the openly accessible DEMs as detailed in [19,20]. In addition to this, the standard deviation of terrain height is computed for the terrain using ICESat-2 data for the representation of topographic ruggedness.

5. Results and Discussion

Considering the ATL06/ICESat-2 elevation values for 19,755 ICESat-2 footprints as a reference, the mean error (ME), mean absolute error (MAE), and RMSE for TanDEM-X were found as 0.26 m, 12.92 m, and 17.4 m, respectively. Similarly, the ME, MAE, and RMSE for ALOS PALSAR RTC HR DEM were found as 0.20 m, 9.50 m, and 13.88 m, respectively. Thus, for the study site in the higher reaches of Himalayan terrain using ICESat-2 ATL06 products, ALOS PALSAR RTC HR DEM (L-band InSAR product) was found to be more suitable than TanDEM-X 90 m (X-band InSAR product), or any openly accessible datasets for varied applications. The range of elevation values in ICESat-2 in the study area is from 3409.75 m to 5976.31 m alongside the ICESat-2 track ID 325 (Figure 2). Figure 3a–c depicts a similar undulating pattern, as depicted by Figure 2b.

The standard deviation of terrain height values representing terrain ruggedness using ICESat-2 elevation values was found as 432.06 m, which is quite higher than those reported for the younger Himalayan region, such as Dehradun and Kalka, which have standard deviations of 134.79 m and 261.08 m, respectively, as shown in earlier studies [21]. The visualization of the experimental sites on Google Earth and OpenAltimetry 3D viewer shows that the mountain slopes are steep, with a large number of peaks and valleys representing the rugged terrain. The region needs more conservation measures for the stabilization of slopes, which pose challenges to the dwellers and tourists. The recent landslides that impacted the Nugulsari and Batseri villages show the danger posed by the landslides. During the recent landslides, the Batseri Bridge collapsed due to the large boulders that tumbled down from the top of the mountains. Since the surface roughness also controls the energy flow, a special accounting is needed for the balanced rocks including large boulders, which are an important subset of fragile geologic features (FGFs) in specific terrain considering the safety of structures. Figures 2 and 3 can guide the ground survey teams for critical slopes and assist in the decision making for suitable measures for stabilization of slopes or site suitability analysis. The ICESat-2 datasets are extremely useful for transport engineering solutions, which requires surface roughness among its important parameters such as terrain roughness, terrain trafficability, and least-cost path for the analysis.

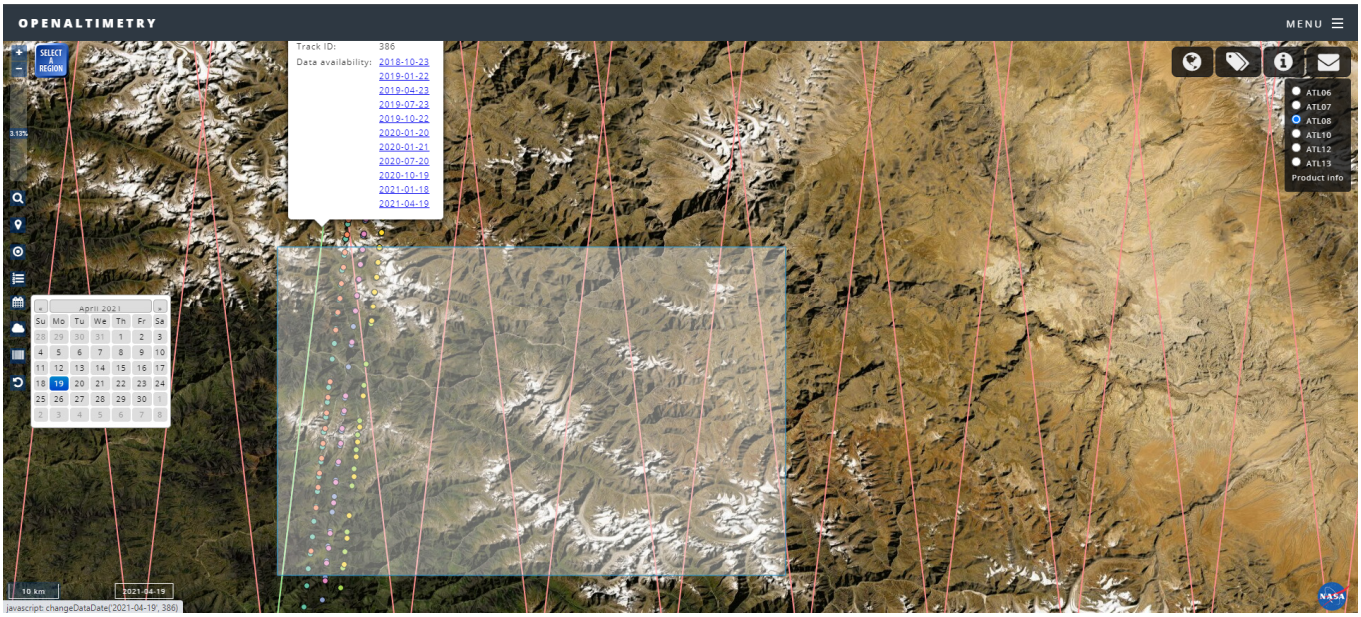

(**a**)

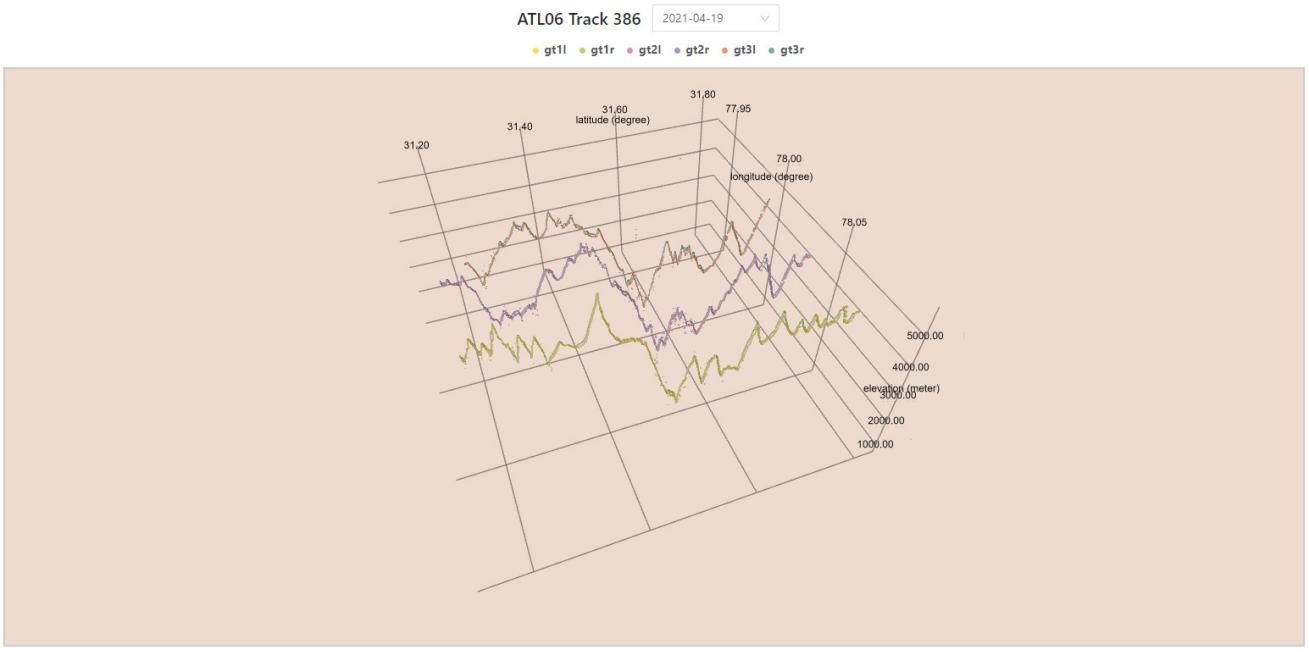

(**b**)

Figure 2. Depicts the study area: (**a**) Parts of Kinnaur District, Himanchal Pradesh, and surroundings overlaid with ICESat-2 footprints; (**b**) Show the OpenAltimetry 3Dviewer describing the terrain cross-sections along the ICESat-2 ground track at footprint/beam locations.

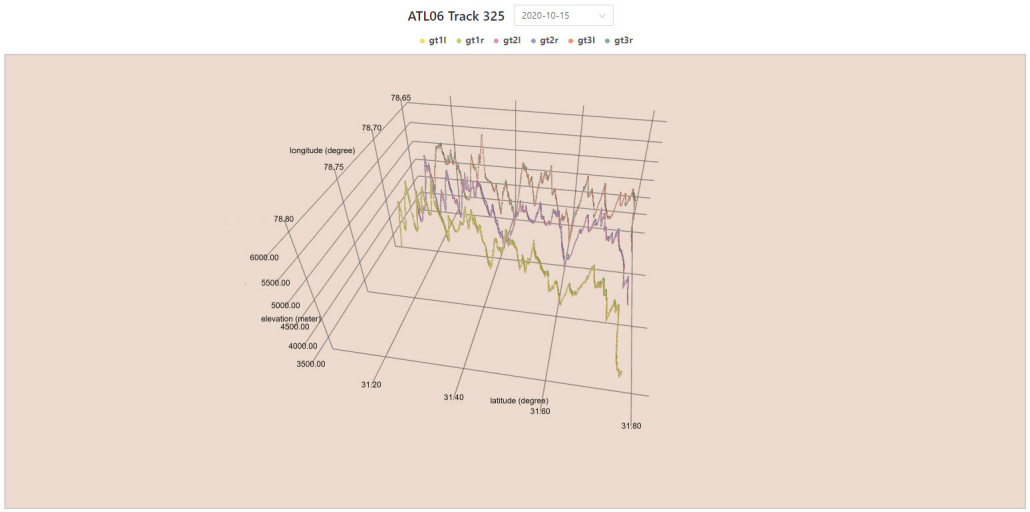

(**a**)

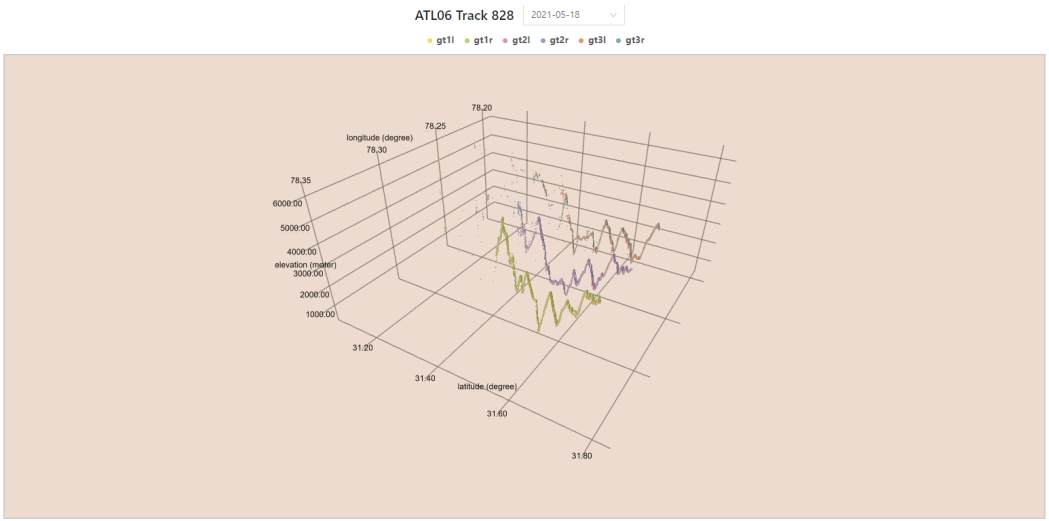

(**b**)

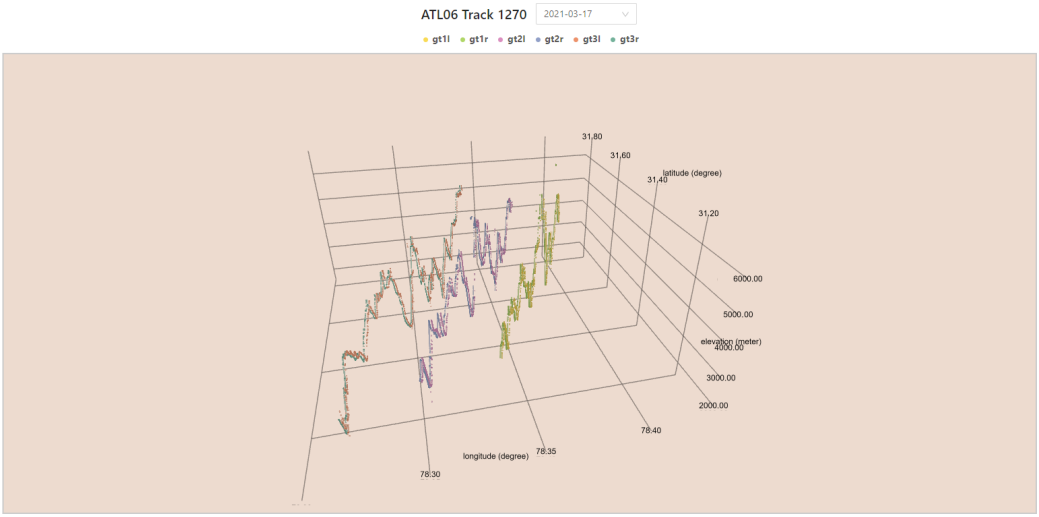

(**c**)

Figure 3. Show the OpenAltimetry 3Dviewer describing the terrain cross-sections along the ICEsat-2 ground track at footprint/beam locations for: (**a**) Track 325; (**b**) Track 828; (**c**) Track 1270.

The study suggests that the locations near drainage lines shall be kept free from habitation as they have more erosion and have chances of rockslides or debris flows as experienced in the past due to high slopes. The rugged regions should be marked for such regions prone to landslides so that the commuters can avoid these routes during rains. During rains, the pore pressure increases and increases the chances of rain-induced landslides. A mechanism can be made for the stabilization of known sensitive landslide-prone areas and marking through regular monitoring of sensitive spots in the changing landscape with time. The regulated control on the movement of vehicles can also reduce pressure on the sensitive zones during monsoon season when there are higher probabilities of rainfall-triggered landslides.

6. Conclusions

L-band ALOS PALSAR RTC HR DEM is found better than the TanDEM-X 90 DEM using the ICESat-2 footprints as a reference due to its high penetration capability, as well as its higher resolution (point posting). The L-band ALOS PALSAR RTC HR DEM is more suitable for any application as compared to the other openly accessible InSAR-based DEMs, such as the TanDEM-X 90m. Detailed investigations, including geological investigations, will be required for conservation practices in the region for the reduction in landslides due to high slopy mountainous terrain. The terrain ruggedness, which is a measure of surface roughness, is required for the delineation of landform components and units at a local to regional scale. This will have an impact on the developmental planning of a region by understanding the processes among the geomorphological units in the region and must be considered while designing or site suitability assessment for any major structures along an alignment of roads or railways. Timely considerations of FGFs can avert a disaster and help in disaster mitigation.

Funding: This research received no external funding.

Institutional Review Board Statement: Not applicable.

Informed Consent Statement: Not applicable.

Data Availability Statement: The ICESat-2 data, TanDEM-X 90 DEM, and ALOS PALSAR RTC HR DEM datasets are available and can be downloaded from https://openaltimetry.org/, https://tandemx-90m.dlr.de (accessed on 23 July 2021), and https://www.asf.alaska.edu/sar-data/palsar/terrain-corrected-rtc/respectively (accessed on 4 August 2021).

Acknowledgments: The author thanks the space agencies: National Aeronautics and Space Administration (NASA), German Aerospace Center (DLR), and Japan Aerospace Exploration Agency (JAXA) along with the Google Earth platform for their insights and support through data sharing platforms, which are highly valuable and critical in this study. The author is highly indebted to Director, IIRS for encouraging the research studies at the Indian Institute of Remote Sensing.

Conflicts of Interest: The author declares no conflict of interest.

References

1. Simeoni, L.; Ronchetti, F.; Costa, C.; Joris, P.; Corsini, A. Redundancy and coherence of multi-method displacement monitoring data as key issues for the analysis of extremely slow landslides (Isarco valley, Eastern Alps, Italy). *Eng. Geol.* **2020**, *267*, 105504. [CrossRef]
2. Palladino, M.R.; Viero, A.; Turconi, L.; Brunetti, M.T.; Peruccacci, S.; Melillo, M.; Luino, F.; Deganutti, A.M.; Guzzetti, F. Rainfall thresholds for the activation of shallow landslides in the Italian Alps: The role of environmental conditioning factors. *Geomorphology* **2018**, *303*, 53–67. [CrossRef]
3. Martha, T.R. *Detection of Landslides by Object-Oriented Image Analysis*; University of Twente: Enschede, The Netherlands, 2011.
4. Martha, T.R.; Roy, P.; Mazumdar, R.; Govindharaj, K.B.; Kumar, K.V. Spatial characteristics of landslides triggered by the 2015 Mw 7.8 (Gorkha) and Mw 7.3 (Dolakha) earthquakes in Nepal. *Landslides* **2017**, *14*, 697–704. [CrossRef]
5. Pánek, T.; Schönfeldt, E.; Winocur, D.; Březný, M.; Šilhán, K.; Chalupa, V.; Korup, O. Moraines and marls: Giant landslides of the Lago Pueyrredón valley in Patagonia, Argentina. *Quat. Sci. Rev.* **2020**, *248*, 106598. [CrossRef]
6. Alcaraz Tarragüel, A.; Krol, B.; van Westen, C. Analysing the possible impact of landslides and avalanches on cultural heritage in Upper Svaneti, Georgia. *J. Cult. Herit.* **2012**, *13*, 453–461. [CrossRef]

7. Wang, C.; Zhu, X.; Nie, S.; Xi, X.; Li, D.; Zheng, W.; Chen, A.S. Ground elevation accuracy verification of ICESat-2 data: A case study in Alaska, USA. *Opt. Express* **2019**, *27*, 38168–38179. [CrossRef] [PubMed]
8. Chen, C.; Yang, S.; Li, Y. Accuracy Assessment and Correction of SRTM DEM Using ICESat/GLAS Data under Data Coregistration. *Remote Sens.* **2020**, *12*, 3435. [CrossRef]
9. Zhang, Y.; Pang, Y.; Cui, D.; Ma, Y.; Chen, L. Accuracy Assessment of the ICESat-2/ATL06 Product in the Qilian Mountains Based on CORS and UAV Data. *IEEE J. Sel. Top. Appl. Earth Obs. Remote Sens.* **2021**, *14*, 1558–1571. [CrossRef]
10. Liu, Z.; Zhu, J.; Fu, H.; Zhou, C.; Zuo, T. Evaluation of the Vertical Accuracy of Open Global DEMs over Steep Terrain Regions Using ICESat Data: A Case Study over Hunan Province, China. *Sensors* **2020**, *20*, 4865. [CrossRef] [PubMed]
11. Wood, J.L.; Harrison, S.; Reinhardt, L. Landslide inventories for climate impacts research in the European Alps. *Geomorphology* **2015**, *228*, 398–408. [CrossRef]
12. USGS. Landslide Hazards. Available online: https://www.usgs.gov/natural-hazards/landslide-hazards/science/landslides-101?qt-science_center_objects=0#qt-science_center_objects (accessed on 14 August 2021).
13. Gracheva, R.; Golyeva, A. Landslides in Mountain Regions: Hazards, Resources and Information. *Geophys. Hazards* **2009**, 249–260. [CrossRef]
14. Martha, T.R.; Roy, P.; Jain, N.; Kumar, K.V.; Reddy, P.S.; Nalini, J.; Sharma, S.V.S.P.; Shukla, A.K.; Rao, K.H.V.D.; Narender, B.; et al. Rock avalanche induced flash flood on 07 February 2021 in Uttarakhand, India—A photogeological reconstruction of the event. *Landslides* **2021**, *18*, 2881–2893. [CrossRef]
15. Pandey, P.; Chauhan, P.; Bhatt, C.M.; Thakur, P.K.; Kannaujia, S.; Dhote, P.R.; Roy, A.; Kumar, S.; Chopra, S.; Bhardwaj, A.; et al. Cause and Process Mechanism of Rockslide Triggered Flood Event in Rishiganga and Dhauliganga River Valleys, Chamoli, Uttarakhand, India Using Satellite Remote Sensing and in situ Observations. *J. Indian Soc. Remote Sens.* **2021**, *49*, 1011–1024. [CrossRef]
16. Meena, S.R.; Bhuyan, K.; Chauhan, A.; Singh, R.P. Snow covered with dust after Chamoli rockslide: Inference based on high-resolution satellite data. *Remote Sens. Lett.* **2021**, *12*, 704–714. [CrossRef]
17. Guth, P.L.; Geoffroy, T.M. LiDAR point cloud and ICESat-2 evaluation of 1 second global digital elevation models: Copernicus wins. *Trans. GIS* **2021**, *25*, 2245–2261. [CrossRef]
18. Saini, O.; Bhardwaj, A.; Chatterjee, R.S. Analysis of Back-Scattering Coefficient of NovaSAR-1 S-Band SAR. In Proceedings of the National Seminar on Recent Advances in Geospatial Technology and Application, Dehradun, India, 2 March 2020; pp. 117–122.
19. Bhardwaj, A. Assessment of Vertical Accuracy for TanDEM-X 90 m DEMs in Plain, Moderate, and Rugged Terrain. *Proceedings* **2019**, *24*, 8. [CrossRef]
20. Saini, O.; Bhardwaj, A.; Chatterjee, R.S. Generation of Radargrammetric Digital Elevation Model (DEM) and Vertical Accuracy Assessment using ICESat-2 Laser Altimetric Data and Available Open-Source DEMs. In Proceedings of the 39th INCA International Congress on New Age Cartography and Geospatial Technology, Digital, India, 18–20 December 2019; p. 12.
21. Bhardwaj, A. Evaluation of openly Accessible MERIT DEM for vertical accuracy in different topographic regions of India. In Proceedings of the 39th INCA International Congress on New Age Cartography and Geospatial Technology, Digital, India, 18–20 December 2019; pp. 1–9.